 © 2007 The Chemical Society of Japan

Energy-Transfer Mechanism in Photoluminescent Terbium(III) Complexes Causing Their Temperature-Dependence

Shinya Katagiri,[1] Yasunori Tsukahara,*[1] Yasuchika Hasegawa,[2] and Yuji Wada*[1,3]

[1]Graduate School of Engineering, Osaka University, 2-1 Yamadaoka, Suita, Osaka 565-0871

[2]Graduate School of Material Science, Nara Institute of Science and Technology, 8916-5 Takayama-cho, Ikoma 630-0192

[3]Department of Applied Chemistry, Graduate School of Natural Science and Technology, Okayama University, 3-1-1 Tsushima-Naka, Okayama 700-8530

Received October 27, 2006; E-mail: yuji-w@cc.okayama-u.ac.jp

Photoluminescence of Terbium(III) complexes was investigated as a function of temperatures in the range of 80–280 K for $[Tb(bfa)_3(H_2O)_2]$ (bfa: 4,4,4-trifluoro-1-phenyl-1,3-butanedionato), $[Tb(hfa)_3(H_2O)_3]$ (hfa: hexafluoroacetylacetonato), $[Tb(tfa)_3(H_2O)_2]$ (tfa: trifluoroacetylacetonato), $[Tb(acac)_3(H_2O)_3]$ (acac: acetylacetonato), and $[Tb(hfa)_3(tppo)_2]$ (tppo: triphenylphosphine oxide). These complexes were classified into the two groups with different temperature-dependences. The first group consisting of $[Tb(bfa)_3(H_2O)_2]$, $[Tb(tfa)_3(H_2O)_2]$, and $[Tb(acac)_3(H_2O)_3]$ showed a dependence determined by the energy gap between the excited triplet state of the ligand and the emitting level of terbium(III) ion. In contrast, for $[Tb(hfa)_3(H_2O)_3]$ and $[Tb(hfa)_3(tppo)_2]$ containing hfa as a ligand, not only the energy gap but also the energy barriers of the "Forward energy transfer" from the ligand to terbium(III) ion and "Back energy transfer" from terbium(III) ion to the ligand were taken into account for understanding their dependences. These results are discussed based on the re-orientation of the complexes accompanied by the forward and back energy transfer processes using DFT calculations.

Lanthanide ions have been extensively investigated due to their superior emission properties.[1–6] Their special emission properties are attributed to optical transitions within the f manifold. The f-electrons are well shielded by the 5s, 5p-orbitals from the chemical environments and therefore retain most of their atomic characters. As a consequence, the spectral positions of the emission lines are almost independent of the surroundings, and the emission spectra as well as the absorption spectra consist of extremely sharp lines. Thus, lanthanide ions have been applied as the luminescent materials. However, f–f transitions are forbidden by odd parity and many of them are also spin forbidden.[7] So, lanthanide ions have the weak absorption. Therefore, many studies have focused on photosensitized emission of lanthanide complexes in order to overcome the weak absorption due to the forbidden f–f transition. Candidates for the photosensitizer are organic molecules and inorganic compounds. Lanthanide complexes having organic ligands have been selected as a photosensitizer, and a zeolite system encapsulating a photosensitizer and lanthanide ions has been also reported as a photosensitization system showing special rainbow colored-emission.[8] Luminescent lanthanide materials are applied for a display and lighting apparatus. Furthermore, europium chalcogenides have been examined as semiconductors, since they are expected for practical applications as recording mediums, LASER devices and photoisolators.[9,10]

Functional probe molecules to measure temperatures/pressures of material surfaces with no-contact are desired for studies on fluid dynamics, aeronautical engineering, environment engineering, and energy technology[11] so that two-dimensional or multi-dimensional mapping of temperatures and pressures in real time can be achieved with no contact measurements. The first luminescent dyes having temperature-sensing property have been reported by Demas and DeGraff in 1988.[12] rhenium complexes,[13,14] ruthenium complexes,[15] platinum complexes,[16] and metal–porphyrins have also been employed as the temperature-sensing probe molecules.[17]

Lanthanide complexes are suitable as non-contact sensing molecules, because of the strong and sharp emission with a long lifetime.[18] However, normally the f–f electrons are well shielded by the 5s, 5p-orbitals from the chemical environment, so the lanthanide compounds are less affected by their environments. Therefore, a strategy for making the temperature sensitivity is required, and the chemical structures of ligands play important roles in the strategy.

Amao and co-workers have reported the first temperature-sensitive dye using europium(III) complexes in 2003.[19] They have prepared a thin film containing (1,10-phenanthroline)tris-[4,4,4-trifluoro-1-(2-thienyl)-1,3-butanedionato]europium(III) ($[Eu(tta)_3(phen)]$) by the Langmuir–Blodgett technique composed of poly(*N*-dodecylacrylamide) (pDDA). The temperature-sensitivity of the europium(III) complex in the polymer film has been reported to be 0.78% $^\circ C^{-1}$. Recently, Khalil et al. also have prepared the high-performance europium(III) complex for temperature sensitive paint (TSP) in 2004 (temperature-sensitivity: 4.42% $^\circ C^{-1}$).[20] Khalil et al. have used thenoyltrifluroacetone, 1,1,1-trimethyl-5,5,6,6,7,7,7-heptafluoro-2,4-heptanedione, 1-phenanthren-3-yl-3-phenanthren-9-yl-pro-

Published on the web August 10, 2007; doi:10.1246/bcsj.80.1492

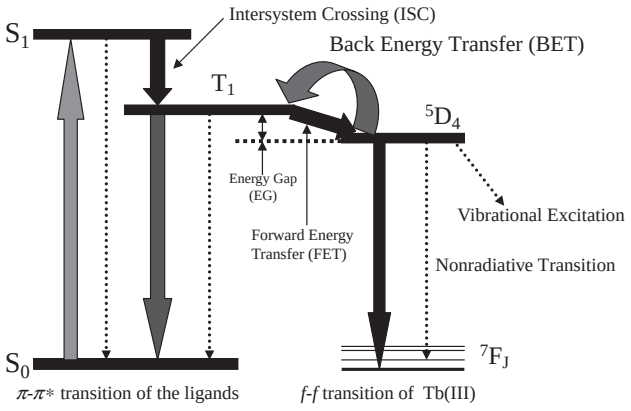

Scheme 1. Energy diagram of terbium(III) complex showing the energy-transfer processes.

pane-1,3-dione, and 4,4,5,5,6,6,6-heptafluoro-1-phenanthren-3-ylhexane-1,3-dione as the ligands. They have measured the decay lifetimes of the emission as a function of temperatures from the three view points: (i) the type and number of ligands in the complex, (ii) the chemical structures of the matrix, and (iii) the concentrations of the europium complexes in the polymer matrix. The origin of the temperature sensitivity in these works is ascribed to changes in the vibrational excitation depending on the temperatures.

We have proposed a terbium(III) complex as a temperature-sensing probe functioning on a mechanistic base of the back energy transfer from the emitting level of terbium(III) ion to the excited triplet state of the ligand (abbreviated as BET) in 2004.[21] The mechanism is schematically shown in Scheme 1. The photosensitized emission is initiated by the excitation of the ground state of the ligand containing a photosensitizer to its excited singlet state (π–π^* transition), followed by intersystem crossing to the excited triplet state. Then, the excitation energy of the excited triplet state is transferred to the lanthanide ions, resulting in the emission. The right side of Scheme 1 shows the 4f orbital of terbium(III) ion. The most important step in this process should be the energy transfer between the excited triplet state (T_1) and the emitting level of terbium(III) ion ($^5D_4$).[22,23] In general, the energy transfer between the excited triplet state of the ligand and the emitting level of Tb ion is described by the Dexter mechanism.[24] The excited energy of terbium(III) ion is dissipated in the two processes; the radiative transition and the nonradiative transition. The nonradiative transition consists of the vibrational excitation, BET and the concentration quenching.[20]

Temperature-dependence is expected for the vibrational excitation and BET in the nonradiative transition from the $^5D_4$ level of terbium(III) ion. However, most of the works using the temperature-sensing molecules have been carried out in the temperature range of 273–330 K. We need to understand the relation of BET and the energy gap (EG) between the excited triplet state of the ligand and the emitting level of terbium(III) ion by investigating the emission properties in a wider range including ultracold temperatures. The systematic measurements of the emission quantum yields of the lanthanide complexes having β-diketone as a ligand from ultracold temperature (77 K) to 300 K have been carried out in 1970 by Sato and Wada.[25] They have reported that the energy-transfer rate becomes larger when the excited triplet state of the ligand is closer to the emitting level of terbium(III) ion, resulting in the increase of the emission quantum yield. However, the EG value that gives the maximum emission quantum yield is not zero but has a certain value. Contribution of BET becomes more, leading to a decrease in the emission quantum yield, when the excited triplet state of the ligand is closer to the emitting level of terbium(III) ion, if BET is considered. Therefore, a suitable EG value giving the maximum emission quantum yield should be determined by both EG and contribution of BET. Furthermore, due to the temperature-dependence of BET caused by an energy barrier present in this process, the suitable EG value giving the maximum emission quantum yield should be changed with the temperature change. Since the emission quantum yield increases with decreasing temperatures due to the less contribution of BET at low temperatures, the maximum value of the emission quantum yield should be observed at a certain value of EG, which should change with respect to temperature.

In the present work, we investigated five terbium(III) complexes with different ligands and show the different temperature-dependent changes in the photosensitized emission properties from the ultracold temperature of 80 to 280 K. We observed the emission spectra and the emission lifetimes and obtained the branching ratios of the five complexes at various temperatures, and we discuss the changes of the symmetry of the complex structures depending on the temperatures in relation to the transition probability of each emission bands of terbium(III) ion ($^5D_4 \rightarrow {}^7F_J$: $J = 0, 1, 2, 3, 4, 5, 6$). The radiative rate could be compared among the complexes from the emission lifetimes at the ultracold temperature (80 K), because BET was fully suppressed at ultracold temperature. In addition, we proposed another factor causing the temperature sensitivity in addition to BET, which is "forward energy transfer," or the energy transfer from the excited triplet ligand to terbium(III) ion. We carried out the quantum chemical calculations of the ligand in the ground state and in the excited triplet state and clarified the origin of the energy barriers present in the forward and back energy transfer processes. Thus, we can fully explain the temperature-dependence of the emission properties of the complexes systematically, and this will contribute to the design of the lanthanide complexes for the controlled temperature-dependent emission.

Experimental

Materials. Terbium(III) acetate tetrahydrate (99.9%), terbium(III) chloride hexahydrate, 1,1,1,5,5,5-hexafluoro-2,4-pentanedione (HFA), triphenylphosphine oxide (TPPO), and 4,4,4-trifluoro-1-phenyl-1,3-butanedione (BFA) were purchased from Wako Pure Chemical Industries Ltd. Isopentane, diethyl ether, and ethanol were obtained from NACALAI TESQUE, INC. Trifluoroacetylacetone (TFA) and acetylacetone (acac) were purchased from TOKYO KASEI KOGYO CO., LTD. They were used for the experiments as supplied.

Apparatus. Infrared spectra used to identify the synthesized materials were obtained with a Perkin-Elmer FT-IR 2000 spectrometer. Elemental analyses were performed with a Perkin-Elmer 240C. ^{19}F NMR data were obtained with a JEOL EX-270 spectrometer. ^{19}F NMR chemical shifts were determined using hexafluorobenzene as an external standard (δ −162.0 (s, Ar–F)).

Preparation of Terbium(III) Complexes. Preparation of Triaquatris(hexafluoroacetylacetonato)terbium(III) ([Tb(hfa)$_3$(H$_2$O)$_3$]): Terbium(III) acetate tetrahydrate (5.0 g, 12.3 mmol) was dissolved in distilled water (20 mL) by stirring. 1,1,1,5,5,5-Hexafluoro-2,4-pentanedione (7 g, 33.6 mmol) was added dropwise to the above solution. The mixture produced a precipitation of white green powder after stirring for 3 h. The reaction mixture was filtered. The resulting white green needle crystals were recrystallized from methanol/water.[7,26] Yield: 70%. IR(KBr): 1650 (st, C=O), 1255–1141 (st, C–F) cm^{-1}. ^{19}F NMR (CD$_3$-COCD$_3$) δ −61.22 (s, CF$_3$). Anal. Calcd for C$_{15}$H$_9$F$_{18}$O$_9$Tb: C, 21.60; H, 1.09%. Found: C, 21.47; H, 1.34%.

Preparation of Tris(hexafluoroacetylacetonato)bis(triphenylphosphine oxide)terbium(III) ([Tb(hfa)$_3$(tppo)$_2$]): Methanol (50 mL) containing [Tb(hfa)$_3$(H$_2$O)$_2$] (1.64 g, 2.04 mmol) and triphenylphosphine oxide (TPPO) (1.22 g, 4.38 mmol) was refluxed under stirring for 12 h. The reaction mixture was concentrated using a rotary evaporator. Reprecipitation by addition of excess hexane produced crude crystals, which were washed in toluene several times. Recrystallization from hot methanol gave green translucent crystals of [Tb(hfa)$_3$(tppo)$_2$].[9] Yield: 56%. Anal. Calcd for C$_{51}$H$_{33}$F$_{18}$O$_8$P$_2$Tb: C, 45.83; H, 2.49%. Found: C, 45.58; H, 2.49%.

Preparation of Tris(acetylacetonato)triaquaterbium(III) ([Tb(acac)$_3$(H$_2$O)$_3$]): Terbium(III) acetate tetrahydrate (5.0 g, 12.3 mmol) was dissolved in distilled water (20 mL) by stirring. 2,4-Pentanedione (3.74 g, 37.4 mmol) was added dropwise to the above solution. The pH value of this solution was adjusted at pH 7 by adding NH$_3$ aqueous solution. The mixture produced a white precipitate after stirring for 3 h. The reaction mixture was filtered. The resulting white needle crystals were recrystallized from methanol/water.[27] Yield: 50%. Anal. Calcd for C$_{15}$H$_{27}$O$_9$-Tb: C, 35.31; H, 5.33%. Found: C, 35.66, H, 5.23%.

Preparation of Diaquatris(benzoyltrifluoroacetylacetonato)-terbium(III) ([Tb(bfa)$_3$(H$_2$O)$_2$]): To ethanol (15 mL) were added 4,4,4-trifluoro-1-phenyl-1,3-butanedione (BFA) (0.65 mg, 3.0 mmol), and then sodium hydroxide (1 M, 3 mL). The mixture was heated to 60 °C and stirred. This solution was dropped into water (10 mL) containing terbium(III) chloride hexahydrate (0.39 g, 1.04 mmol). Ethanol in the mixture was removed by evaporation after stirring for 3 h. White-yellow powder was obtained. The reaction mixture was filtered, and the powder was purified with ethanol/water.[27] Yield: 34%. Anal. Calcd for C$_{30}$H$_{22}$F$_9$O$_8$Tb: C, 42.87; H, 2.64%. Found: C, 42.73, H, 2.62%.

Preparation of Diaquatris(trifluoroacetylacetonato)terbium(III) ([Tb(tfa)$_3$(H$_2$O)$_2$]): Terbium(III) acetate tetrahydrate (3.78 g, 8.3 mmol) was dissolved in distilled water (30 mL) by stirring. Trifluoroacetylacetone (4.07 g, 26.4 mmol) was added dropwise to the above solution. The mixture was heated to 60 °C and stirred. The mixture produced a white green precipitate after stirring for 5 h. The reaction mixture was filtered. The resulting white needle crystals were recrystallized in methanol/water.[7,26] Yield: 64%. Anal. Calcd for C$_{15}$H$_{16}$F$_9$O$_8$Tb: C, 27.54; H, 2.47%. Found: C, 27.44; H, 2.40%.

Optical Measurements. The emission spectra were measured on a SPEX-Fluorolog τ-3 (JOBIN YVON) system equipped with low-temperature options. Low temperatures were achieved by means of a nitrogen bath cryostat (Oxford Instruments, Optistat DN) and a temperature controller (Oxford Instruments, ITC 502S) (80–300 K). The excitation spectra were measured by HITACHI F-4500 spectrophotometer. The absorption spectra were measured by a JASCO V-570 spectrometer. Decay profiles monitored at 543 nm were recorded with a photomultiplier coupled to a Tektronix TDS3052 oscilloscope upon excitation with the third harmonic of a Nd:YAG laser (355 nm).[9] Each optical measurement was carried out in EPA (ethanol:isopentane:ether = 2:5:5) in the temperature range of 80–280 K using a 1 cm rectangular quartz cell.

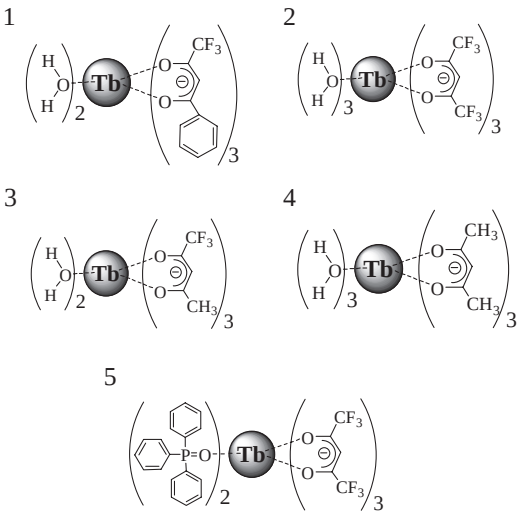

Fig. 1. Chemical structures of **1** = [Tb(bfa)$_3$(H$_2$O)$_2$], **2** = [Tb(hfa)$_3$(H$_2$O)$_3$], **3** = [Tb(tfa)$_3$(H$_2$O)$_2$], **4** = [Tb(acac)$_3$-(H$_2$O)$_3$], and **5** = [Tb(hfa)$_3$(tppo)$_2$].

Table 1. Triplet State Energies of Gd β-Diketonates

Complex	The triplet state energy/cm^{-1}
[Gd(acac)$_3$(H$_2$O)$_3$]	24800
[Gd(tfa)$_3$(H$_2$O)$_2$]	22800[a)]
[Gd(hfa)$_3$(H$_2$O)$_3$]	22200
[Gd(bfa)$_3$(H$_2$O)$_2$]	21400[a)]

a) The value from literature.[25]

Results

Photosensitized Luminescence. The structures of the terbium(III) complexes employed in this work are shown in Fig. 1. We selected β-diketone as a common structure in the ligands, because we were able to control the properties of the complexes by modifying the substituents at both ends of the ligands (4 modified ligands). In Table 1 are listed the levels of the excited triplet states of the 4 ligands determined by measuring the phosphorescence of gadolinium(III) complexes of each ligand.[25] In addition, we synthesized complex **5** by substituting the three coordinating water molecules of complex **2** with triphenylphosphine oxide (TPPO) in order to investigate the effect of the structure of the second ligand on the emission properties. When the EG (expressed as Δ) between the excited triplet state of the ligand and the emitting level of terbium(III) ion are less than $\Delta = 1850\,\text{cm}^{-1}$, BET becomes appreciable at room temperature.[28] hfa of complex **2** has an EG of $\Delta = 1700\,\text{cm}^{-1}$, so BET should be important in the emission. We selected bfa ($\Delta = 900\,\text{cm}^{-1}$) having EG smaller than hfa's, tfa ($\Delta = 2300\,\text{cm}^{-1}$) having EG a little larger than $\Delta = 1850\,\text{cm}^{-1}$, and acac ($\Delta = 4300\,\text{cm}^{-1}$) having a large EG.

The emission spectrum of complex **3** in EPA at 300 K (Fig. 2) was a typical one of a terbium(III) ion. The emission

bands were observed at 490, 545, and 583 nm, attributed to the f–f transitions $^5D_4 \rightarrow {}^7F_6$, $^5D_4 \rightarrow {}^7F_5$, and $^5D_4 \rightarrow {}^7F_4$, respectively. The other complexes were also found to have the typical emission spectrum of a terbium(III) ion.

The excitation spectra of the five terbium(III) complexes at 300 K are shown in Fig. 3. The spectra were monitored at 543 nm, which is attributed to the f–f transition ($^5D_4 \rightarrow {}^7F_5$) of a terbium(III) ion. The peaks of the excitation bands of complexes **1**, **2**, **3**, and **4** were observed at 365, 336, 325, and 315 nm, respectively. The excitation band of complex **5** had a shoulder at 340 nm.

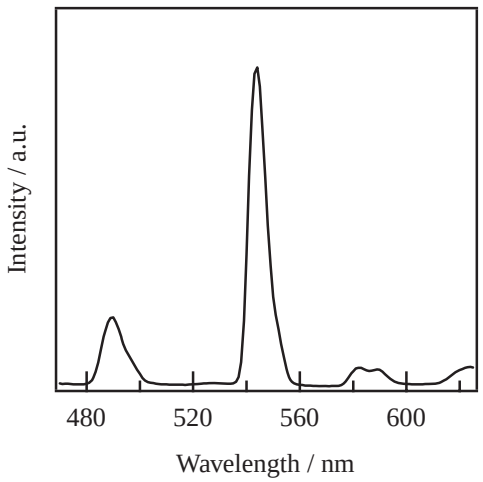

Fig. 2. Emission spectrum of **3** in EPA (ex. at 330 nm) at 300 K (1.02 mM).

The absorption spectra of the five terbium(III) complexes at 300 K are shown in Fig. 4. The π–π^* transitions of the four ligands were observed. Therein, the rising edges of the spectra were located at 375, 360, 340, 330, and 360 nm for complexes **1**, **2**, **3**, **4**, and **5**, respectively. It was concluded from the coincidence between the absorption and the excitation spectra that the emission of terbium(III) ion is induced by the π–π^* absorption of the ligands. Therefore, energy transfer from the excited state of the ligand to terbium(III) ion leading to the photosensitized emission of terbium(III) ion has been confirmed.

Temperature-Dependent Photosensitized Luminescence. The emission spectra of the five terbium(III) complexes were measured over a wide range of temperatures (80–280 K), as shown in Fig. 5. The emission intensities normalized by the intensities at the maxima obtained at 80 K for each complex are plotted against the temperatures in Fig. 6. We abandoned the comparison of the absolute intensities, because we needed to change the slits of the optical measurement set-up for each terbium(III) complex due to widely varied emission intensities of the complexes.

The temperature-dependence of the emission spectrum of complex **1** in EPA is shown in Fig. 5a. The excited triplet state of the bfa was closest to the $^5D_4$ level of terbium(III) ion among the five complexes employed in this work (EG of complex **1** was $\Delta = 900\,\mathrm{cm}^{-1}$). Therefore, the emission of complex **1** should be affected by BET. Actually the emission spectrum of complex **1** was very weak at 180–280 K due to the energy dissipation through BET. The emission intensities of

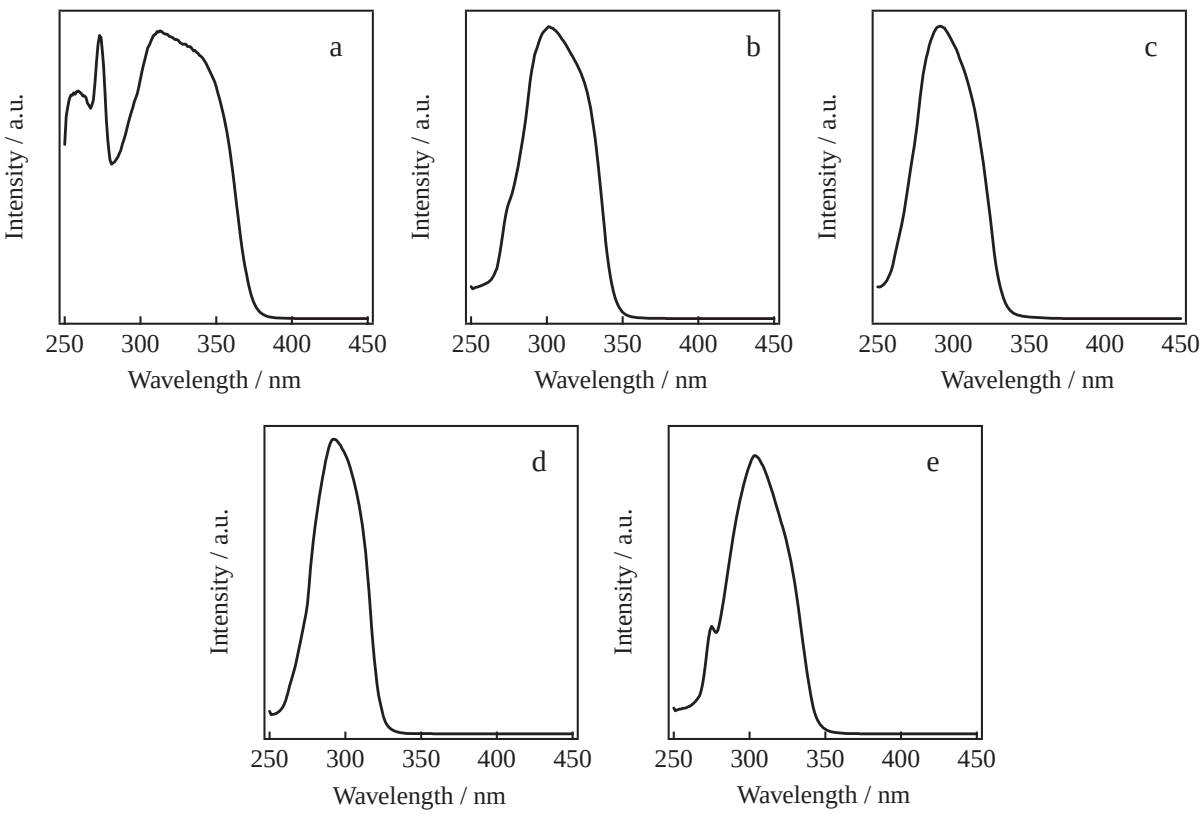

Fig. 3. Excitation spectra of a) **1** (0.014 mM), b) **2** (0.0084 mM), c) **3** (0.011 mM), d) **4** (0.022 mM), e) **5** (0.0067 mM) in EPA at 300 K monitored at 543 nm ($^5D_4 \rightarrow {}^7F_5$).

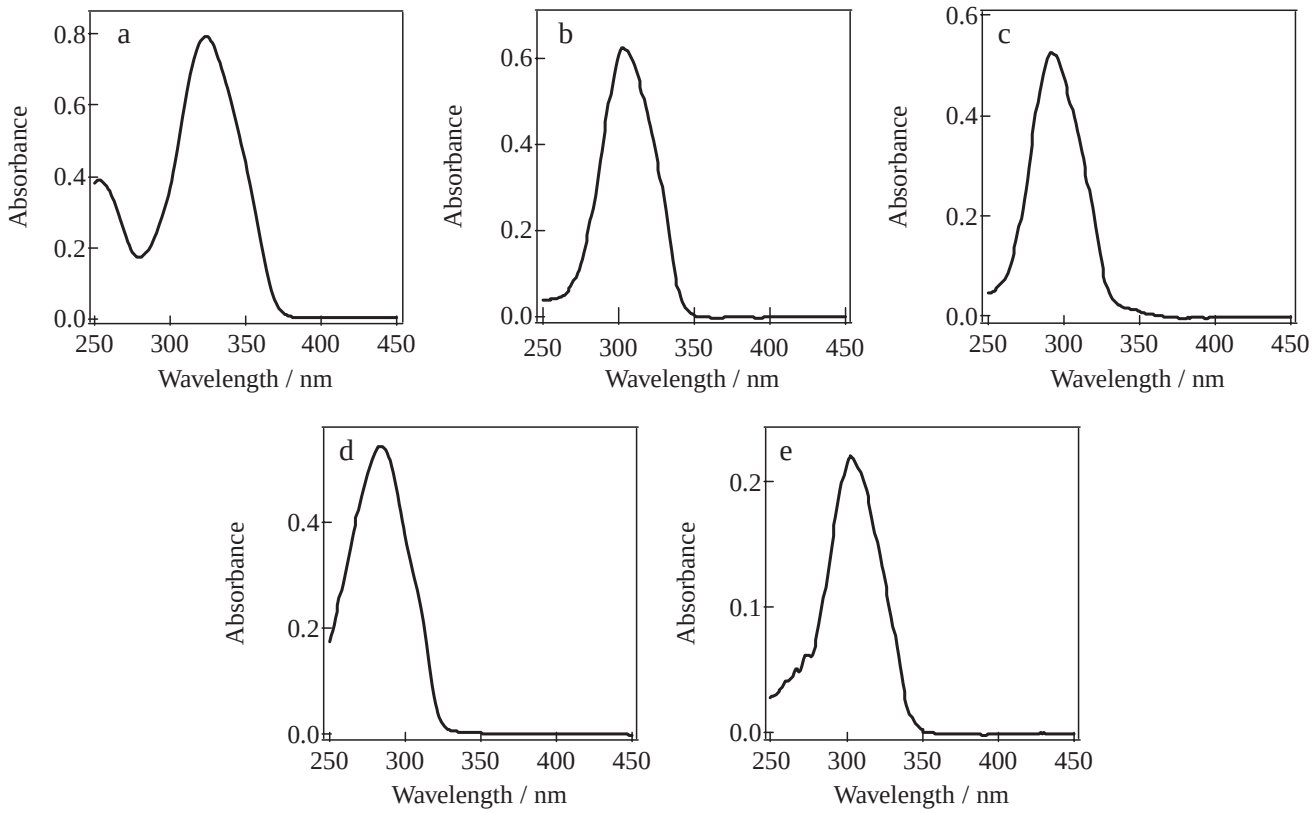

Fig. 4. Absorption spectra of a) **1** (0.014 mM), b) **2** (0.0084 mM), c) **3** (0.011 mM), d) **4** (0.022 mM), e) **5** (0.0067 mM) in EPA at 300 K.

complex **1** dramatically increased with a decrease in the temperature below 160 K (Fig. 6a). This can be understood as a result of the suppression of BET below 160 K.

The emission spectra of complex **2** in EPA depending on temperature are shown in Fig. 5b. BET can occur at room temperature, when it is taken into account that EG of complex **2** is $\Delta = 1700\,\mathrm{cm}^{-1}$. The emission intensity of complex **2** increased in the temperature range from 280 to 240 K and then decreased in the temperature range from 240 to 160 K. We called the change the volcano-shaped. The top of the volcano-shape was located at 240 K (Fig. 6b). The volcano-shape dependence in the emission intensities on the temperatures were observed only for complexes **2** and **5** having hfa as a ligand, and not observed for the complexes **1**, **3**, and **4**. The emission intensities of complex **2** dramatically increased with a decrease in the temperatures below 160 K.

The emission spectra of complex **5** in EPA depending on temperature are shown in Fig. 5e. The change in the emission intensity of complex **5** was also showed the volcano-shaped in the temperature range from 160 to 280 K (Fig. 6e). The temperature-dependences of the complexes **2** and **5** having hfa showed the volcano-shape, as shown in Figs. 6b and 6e.

The temperature-dependence of the emission spectrum of complex **3** in EPA is shown in Fig. 5c. The emission intensities of complex **3** dramatically increased with a decrease in the temperature from 280 to 200 K. The changes of the emission intensity of complex **3** became less below 200 K (Fig. 6c) than above the temperature. The increase observed in the region from 280 to 200 K might be understood as a result of the suppression of BET. However, BET should not be so dominant when EG of $\Delta = 2300\,\mathrm{cm}^{-1}$ was considered. The critical value for the occurrence of BET proposed by Latva et al. seems to vary depending on the structures of the complexes.[28]

The temperature-dependence of the emission spectrum of complex **4** in EPA is shown in Fig. 5d. The spectra were noisy due to weak emission intensities. EG of complex **4** was $\Delta = 4300\,\mathrm{cm}^{-1}$. Therefore, the emission intensity of complex **4** should not be affected by BET. The emission intensity of complex **4** mildly increased with a decrease in temperature. (Fig. 6d) The temperature-dependence of the emission intensity of complex **4** can be understood as a result of the suppression of the vibrational excitation.[29,30]

In summary, the temperature-dependences of the emission intensities of complex **1** and **3** showed drastic effect of BET, i.e., the changes in the emission intensities dramatically increased upon suppression of BET. The results obtained here have led to an important conclusion that the suppression of BET contributes more effectively to the temperature-dependence of the emission intensity of terbium(III) complexes than that of the vibrational excitation.

Lifetime Measurement. We measured the decays of the emission of the five terbium(III) complexes. Time profiles of the $^5D_4 \rightarrow {}^7F_5$ emission (543 nm) of terbium(III) ion were observed, as shown in Fig. 7. The linear decays in the plot of logarithm of the emission intensity against the time were obtained for the complexes giving strong emission, but the fluctuation could not be removed for those giving weak emission. Thus, we used only the initial stages of the profiles for

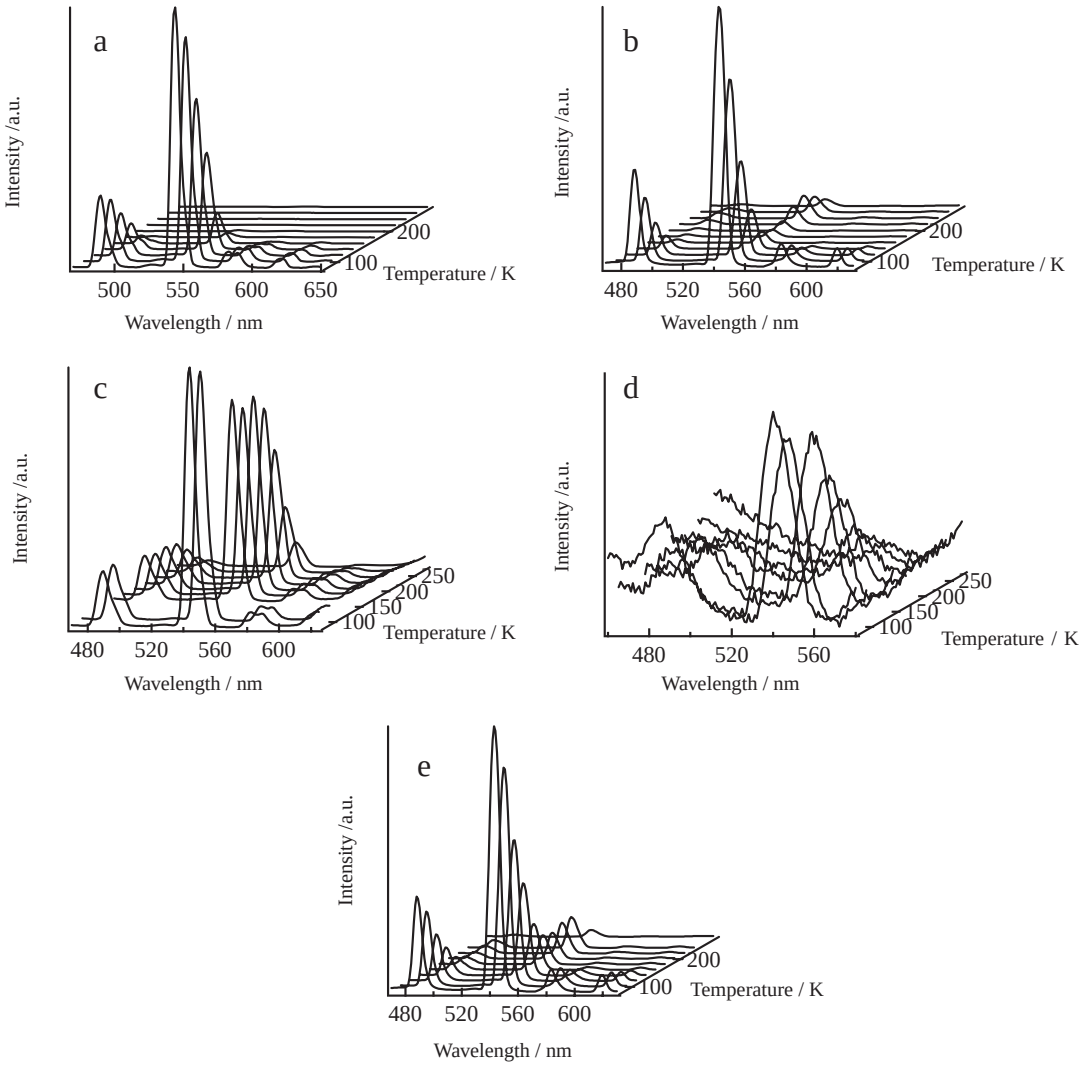

Fig. 5. Temperature-dependence of the emission spectra of a) **1** (Ex. at 365 nm, slit 5 nm for excitation/4 nm for emission), b) **2** (Ex. at 336 nm, slit 5 nm for excitation/5 nm for emission), c) **3** (Ex. at 330 nm, slit 7 nm for excitation/4 nm for emission), d) **4** (Ex. at 315 nm, slit 15 nm for excitation/15 nm for emission), and e) **5** (Ex. at 336 nm, slit 5 nm for excitation/5 nm for emission, in EPA). The concentrations were 15.5 μM for **1**, 16.8 μM for **2**, 18.3 μM for **3**, 13.7 μM for **4**, 16.5 μM for **5**.

obtaining the lifetimes by fitting to the linear dependence. The emission lifetimes of the terbium(III) complexes in EPA are plotted against the temperatures in Fig. 8.

The emission lifetimes of the five terbium(III) complexes at 280 K were spread over a wide range but were similar (around 600–900 μs) at 80 K, at which BET and vibrational excitation should be suppressed. The emission lifetime of complex **2** was largest at 80 K among the five complexes. The emission lifetime of complex **1** was very short without an appreciable change in the temperature range of 180–280 K and greatly increased below 180 K, showing a steady value below 125 K (650 μs). The emission lifetime of complex **2** was very short and did not change in the temperature range of 180–280 K, in contrast to complex **1**. The emission lifetime of complex **2** greatly increased below 150 K. The emission lifetime of complex **3** increased with a decrease in the temperature between 220 and 280 K and slightly changed below 200 K. The emission lifetime of complex **4** did not show a large change and stayed near 800 μs over the whole temperature region. The emission lifetime of complex **5** steadily increased with a decrease in the temperature.

The temperature-dependence of the lifetime of the emission of the terbium(III) complexes can be understood by the contribution of the vibrational excitation and BET depending on temperatures. The temperature-dependence of BET should be related to the energy gap from the $^5D_4$ level of Tb^{III} to the excited triplet state of the ligand. Therefore, the difference observed for the temperature-dependence of the emission lifetimes of the five complexes can be attributed to the different EG values.

Energy transfer from T_1 to the $^5D_4$ level is so fast that we could not observe the gradual rise of emission in Fig. 7. Therefore, the emission lifetime (τ) is given by the following equation:

$$\tau = \frac{1}{k_r + k_{nr}[\mathrm{Tb}] + k_v + k_{BET}}, \quad (1)$$

where k_r, $k_{nr}[\mathrm{Tb}]$, k_v, and k_{BET} are the rate constants of

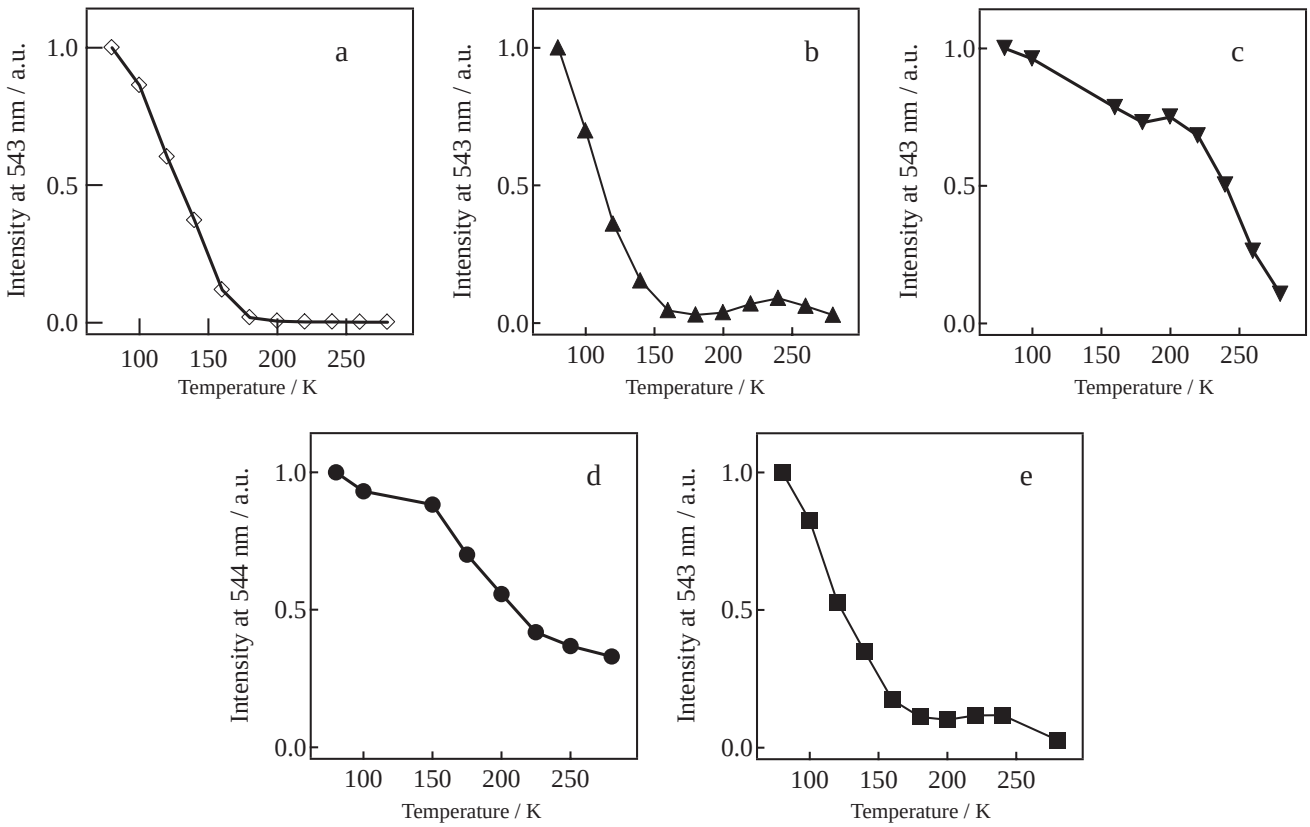

Fig. 6. Temperature-dependence of the emission intensity at 543 nm of a) **1**, b) **2**, c) **3**, d) **4**, and e) **5** in EPA. The emission intensities were normalized by the intensities at the maxima obtained at 80 K for each complex.

radiative transition, concentration quenching, vibrational excitation, and BET, respectively. Here, the emission intensity of Tb nitrate in EPA (excited at 370 nm) was very weak in the temperature range of 80–270 K (Fig. 9). The temperature-dependence of the emission intensity of terbium(III) ion in its nitrate slightly changed, indicating that the temperature-dependence of the f–f transition in terbium(III) ion was negligible as shown in the inset of Fig. 9. Thus, we assume that k_r and k_{nr} are not dependent on the temperatures. From Eq. 1, only k_v and k_{BET} should decrease with a decrease in the temperature. Accordingly, the τ increases. τ is determined mainly by k_{BET}, because the temperature-dependence of k_v in terbium(III) complex is less than that of k_{BET}. Less temperature-dependence of k_v has been described in the section of "Temperature-Dependent Photosensitized Luminescence."

Branching Ratio. In the case of Eu^{III}, the radiative rates of europium(III) complexes are linked to geometric structures.[7] If there is no inversion symmetry at the lanthanide ion sites, uneven ligand-field components can mix with opposite-parity states in $4f^n$-configuration levels. Electric-dipole transitions are then no longer strictly forbidden in the ligand fields, resulting in faster radiative rates.[31] We wish to discuss the radiative rates and the molecular structures of terbium(III) complexes in the same way as europium(III) complex.[9] Thus, the branching ratios evaluated by the emission spectra of the terbium(III) complexes were compared in order to discuss the radiative rates in relation to the symmetry of the ligand fields here again.

The emission spectra of the europium(III) complexes were normalized with respect to the $^5D_0 \rightarrow {}^7F_1$ transition, which is known as a magnetic-dipole transition independent of the changes of the ligand fields. In the case of terbium(III) complex, the referential peaks chosen were the $^5D_4 \rightarrow {}^7F_5$ (543 nm) and $^5D_4 \rightarrow {}^7F_6$ transition (488 nm), corresponding to the magnetic-dipole transition ($^5D_4 \rightarrow {}^7F_5$) of $\Delta J = 1$ and the electric-dipole transition ($^5D_4 \rightarrow {}^7F_6$) of $\Delta J = 2$, respectively. Here, the spectra were normalized with respect to the $^5D_4 \rightarrow {}^7F_5$ transition corresponding to the magnetic-dipole transition being independent of the ligand fields. The branching ratio was defined as that of the intensity of the electric-dipole transition to the magnetic-dipole transition. Asymmetry of the ligand field is reflected as increase in the branching ratio, resulting in increase in the radiative rate.[7]

The emission spectra of complex **3** normalized with respect to the magnetic dipole transition at 80, 100, 200, and 280 K are shown in Fig. 10C. No change in the branching ratios was observed at these different temperatures. So, the ligand field should not be changed by changing the temperature. Therefore, k_r should be independent of the temperatures. The branching ratios for complexes **1** and **4** did not show any change with the change in the temperature as well as for complex **3** (Figs. 10A, 10C, and 10D), leading to the same discussion on the ligand field and k_r. Thus, it was concluded that the geometric structures of complex **1**, **3**, and **4** do not change with temperature. On the other hand, though the branching ratios of complex **2** and **5** showed no change in the temperature range of 180–280 K, they increased with a decrease in the temperature below 180 K (Figs. 10B and 10E), indicating the structural change below this temperature.

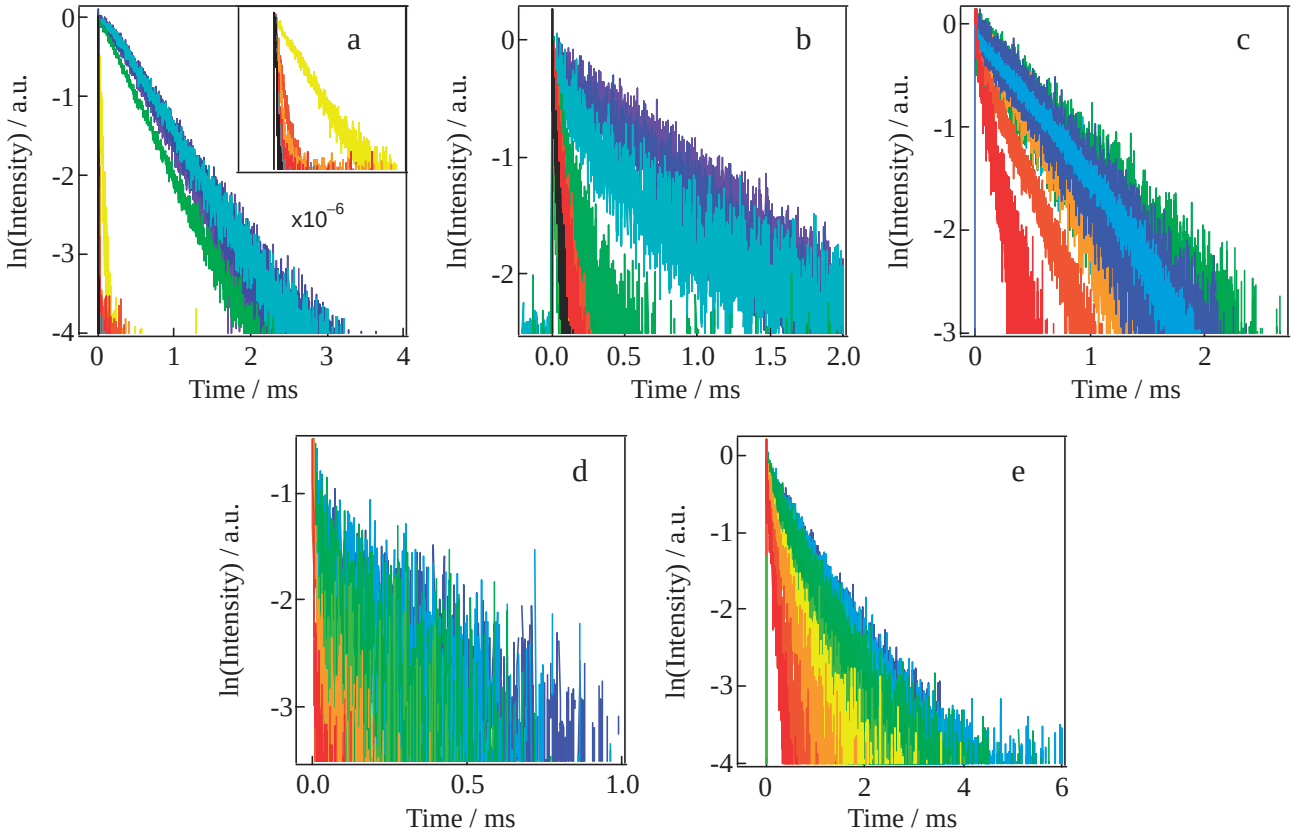

Fig. 7. Temperature-dependence of the emission decay of a) **1** (1.2 mM) (inset: 180–280 K), b) **2** (0.28 mM), c) **3** (1.0 mM), d) **4** (1.3 mM), and e) **5** (1.2 mM) in EPA in the temperature range of 80–280 K.

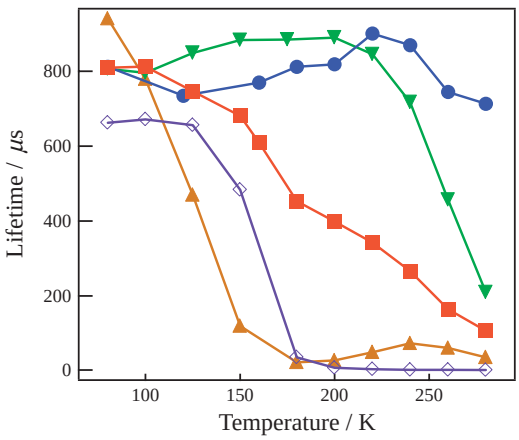

Fig. 8. Temperature-dependence of τ of **1** (◇), **2** (▲), **3** (▼), **4** (●), and **5** (■) in EPA obtained from Fig. 7.

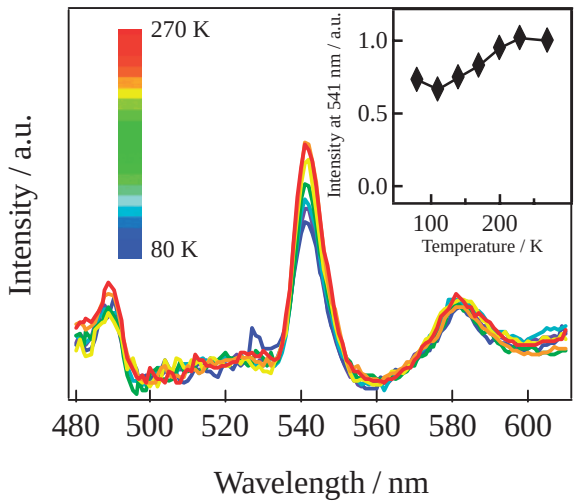

Fig. 9. Emission spectra of $Tb(NO_3)_3$ in EPA (0.063 M) observed between 80 and 270 K, Ex. at 370 nm, slit 5 nm for excitation/5 nm for emission. Inset: Temperature-dependence of the emission intensities observed at 543 nm.

Emission spectra of complexes **1**, **3**, and **4** at 80 K normalized with respect to the $^5D_4 \rightarrow {}^7F_5$ transition in each spectrum are shown in Fig. 11. The order of the branching ratios obtained from Fig. 11 was complex **1** > complex **4** ≒ complex **3**, indicating that the symmetry of these complexes should decrease in this order. Therefore, k_r should increase in this order, because the f–f transition is allowed upon degeneration of the symmetry of the complex structure. Here, when BET is completely suppressed at 80 K, τ of the complexes should be controlled only by k_r from Eq. 1. The order of τ of the complexes at 80 K was complex **3** ≒ complex **4** > complex **1**. Therefore, the order of the value of k_r evaluated from τ was complex **1** > complex **4** ≒ complex **3**, agreeing with the order of k_r estimated from the branching ratio.

We excluded complexes **2** and **5** from the above discussion. Because τ of complexes **1**, **3**, and **4** reached a maximum and

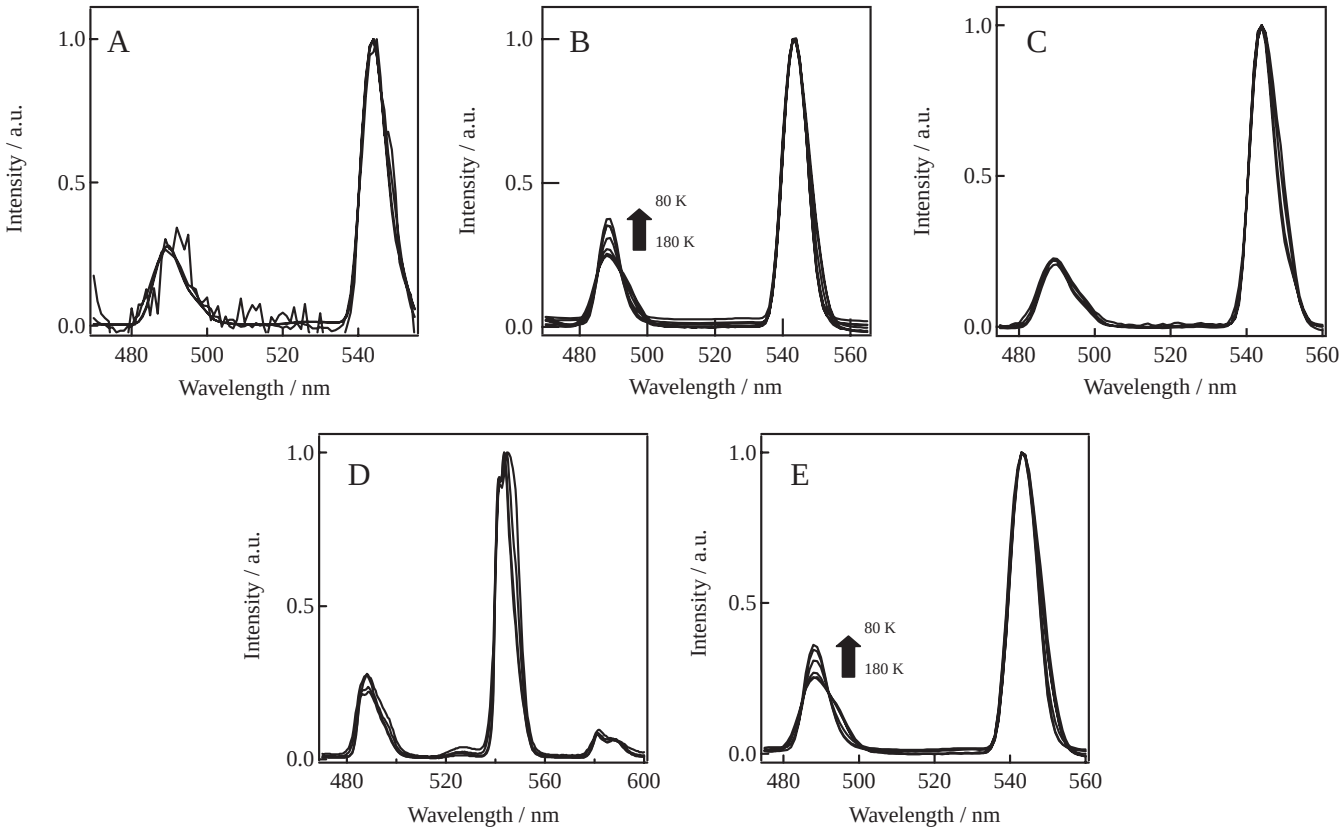

Fig. 10. Emission spectra of the complexes in EPA normalized with respect to the magnetic-dipole transition at various temperatures. A) **1** at 80, 100, 200, and 280 K, B) **2** at 80, 100, 140, 160, 200, 240, and 280 K, C) **3** at 80, 100, 200, and 280 K, D) **4** at 80, 100, 200, and 280 K, and E) **5** at 80, 100, 140, 160, 200, 240, and 280 K. The concentrations were 15.5 μM for **1**, 16.8 μM for **2**, 18.3 μM for **3**, 0.59 mM for **4**, and 16.5 μM for **5**.

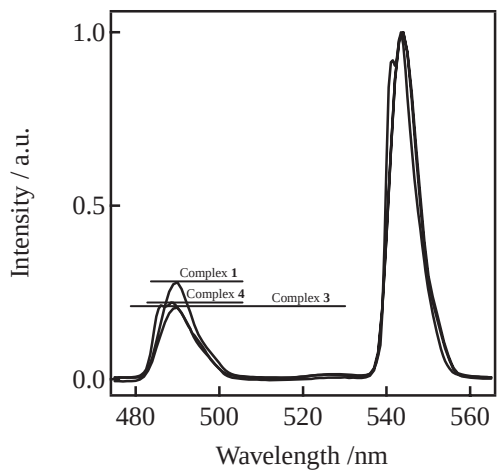

Fig. 11. Emission spectra of complex **1** (15.5 μM), **3** (18.3 μM), and **4** (0.59 mM) at 80 K normalized with respect to the magnetic-dipole transition.

complexes **2** and **5** showed an increasing behavior at 80 K even, BET could still contribute to the emission properties of these two complexes.

Discussion

Dependence of the Emission Lifetimes on the Temperatures. Thermal energy required for BET becomes higher when EG is large, resulting in the suppression of BET at higher temperatures for the complexes having large EG. Therefore, the complexes should undergo suppression of BET in the order of complex **4** > complex **3** > complex **2** = complex **5** > complex **1** when the temperature is decreased. However, EG of complex **4** was very large, and therefore, its emission lifetime should increase above the measurement temperatures employed in this work. No clear increase was observed in the present work.

Since EG determines the temperature at which suppression of BET occurs, the increment in the τ should be in the order of complex **3** > complex **2** > complex **1**. However, the order obtained in the present experiment was complex **3** > complex **1** > complex **2**. The temperature-dependence of the τ expected from EG was observed for complexes **1**, **3**, and **4**, but complex **2** showed unexpected behavior. The rapid increase in the τ was observed from 280 to 220 K for complex **3**, which was attributed to suppression of BET. The increase observed from 180 to 125 K for complex **1** should be also attributed to suppression of BET. An increase in τ was expected from 200–250 K for complex **2** from EG, but a volcano-shaped dependence was observed at this temperature region. In addition, the rapid increase was shifted to the lower temperature region of 80–150 K.

In the previous section, it was shown that the branching ratio observed in the emission of complex **2** having HFA as a ligand increased a with decrease in the temperature, while

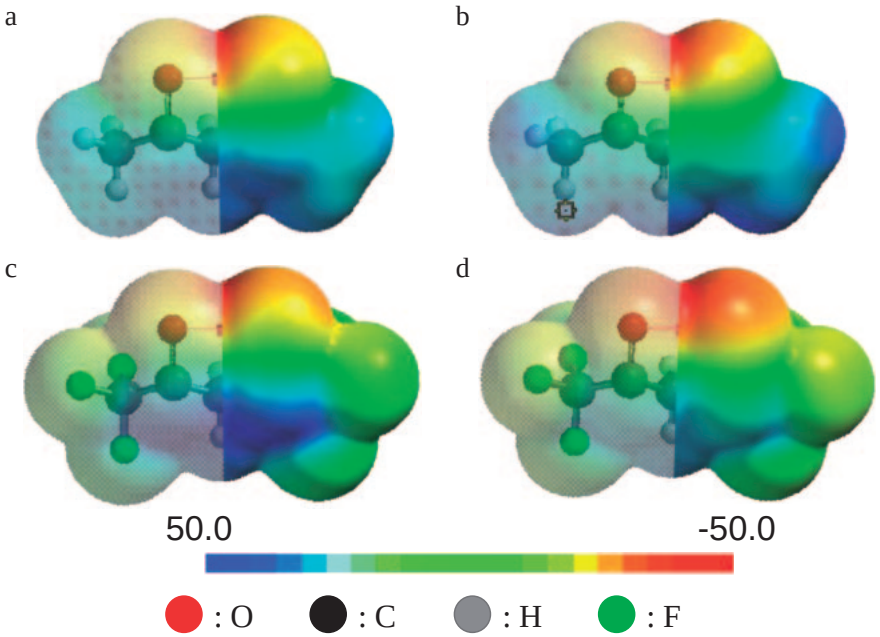

Fig. 12. Three-dimensional electrostatic potential views obtain by DFT calculation. a) the ground state of acac, b) the excited triplet state of acac, c) the ground state of HFA, d) the excited triplet state of HFA. Electrostatic potential map from −50.0 to 50.0 kcal mol^{-1} onto a 0.002 eÅ^{-3}.

those of the other complexes having no HFA did not change by the changes of the temperatures, indicating that the symmetry of complex **2** should change with changes in the temperature. Therefore, the temperature-dependence of τ of complex **2** cannot be explained only by the idea of BET determined by EG.

Unusual Temperature-Dependence of the Emission Property of [Tb(hfa)$_3$(H$_2$O)$_3$]. We explained the temperature-dependence of the photosensitized emission of the terbium(III) complexes by the concept of BET determined by EG as described above. However, we could not explain the behavior of complex **2** having HFA as a ligand. Therefore, we introduce another idea in order to understand the unusual behavior of complex **2**: presence of an energy barrier (EB) in the forward energy transfer (FET) from the excited triplet state to terbium(III) ion. This EB should be related to a change between the starting structure of the complex and the final one, which can be referred as "re-orientation" of the complex induced by FET. This EB should depend on the chemical structures of the ligands.[32]

EB of FET for complex **2** should be large compared to those of the other complexes, resulting in the competitive relation between FET and BET. This should be a reason why only complex **2** showed unusual behavior. In the case of HFA having –CF$_3$ groups with an electron-withdrawing properties, the electron configuration of the ligand is greatly different between the ground state and the excited triplet state. Therefore, the chelating structures of the ligands with a terbium(III) ion should be very different between the two situations as demonstrated by the following section dealing with the quantum chemical calculations.

We carried out DFT calculations on acac (used as a ligand in complex **4**) and HFA (used as a ligand in complex **2**) in the singlet ground state (S_0) and the excited triplet state (T_1). Fully optimized geometries were obtained for the ligands in the ground state at DFT B3LPY/6-31G* levels. Electrostatic potential maps of the two ligands for both in the ground state and the excited triplet state were obtained by a single point calculation at the DFT B3LPY/6-31G* levels on the assumption that the geometries of the ligands in the excited triplet state did not change from those in the ground state. Three-dimensional electrostatic potential views of the two ligands are depicted in Fig. 12 (a: S_0 of acac, b: T_1 of acac, c: S_0 of HFA, d: T_1 of HFA). As shown in Figs. 12c and 12d, there was a large difference in the electrostatic potential between S_0 and T_1 states of the hfa ligand, and it was more dramatic than those seen for acac (Figs. 12a and 12b). The charges of the two O atoms (−0.204) of the hfa ligand in T_1 state was more positive than that in S_0 state (−0.275), indicating a change in the charge distribution caused by the excitation and the intersystem crossing. On the other hand, the charges of the two O atoms (−0.325) of the acac ligand in T_1 state were also more positive than that in S_0 state (−0.345). However, the change in the charges of the O atoms caused by the excitation and the intersystem crossing for the hfa ligand was 0.071, which was larger than that (0.020) for the acac ligand. The above results obtained by the DFT calculations support the following discussion.

In the ground state, the negative charge of the HFA ligand is less localized than in the acac ligand and is extended on the whole molecule. Furthermore, the excitation and the intersystem crossing enhance the delocalization of the charge in the molecules. The induced change of the charge is more dramatic for the hfa ligand than for the acac ligand therein, leading to an idea that the re-orientation energies accompanied with FET and BET are higher for complex **2** than complex **4**, if the re-orientation energies originate mainly from changes in the chelating structures of the complexes. These high re-orientation energies should act as EB present in FET and BET for complex **2**. The barriers should be different from each other for

FET and BET, because the starting structures are different for both processes.

Dependence of the emission lifetimes on temperatures observed for complex **2** was different from that for complexes **1**, **3**, and **4**. The dependence of complex **2** showed a volcano-shape between 200 and 280 K and rapidly increased below 150 K. The branching ratio showed no change between 200 and 280 K, and increased below 200 K, indicating a structural change in complex **2** below this temperature. The volcano-shaped dependence is attributed to the competitive contribution of FET and BET between 200 and 280 K. When the temperature is decreased, suppression of BET first should induce an increase in τ and then that of FET should lead to its decrease, resulting in the volcano-shape. A rapid increase in the emission lifetime observed below 150 K is related to the changed chelating structure of complex **2**, which was confirmed by the discussion of the change of the branching ratio.

On the other hand, in the case of complexes **1**, **3**, and **4**, the re-orientation energy should be small, because they possess methyl group or a phenyl group, which is less electron-withdrawing than $-CF_3$. Accordingly, EB is small. So, the temperature-dependence of complexes **1**, **3**, and **4** should be controlled mainly by BET. Thus, the results were understandable from EG for these complexes. For complex **5**, the second ligands were bulky. So, the re-orientation should need more thermal energy. In consequence, the suppression of BET appeared in the whole range temperature.

Conclusion

We observed the temperature-dependence of the photosensitized emission of terbium(III) complexes having β-diketonato ligands systematically varied in their structures over a wide range of temperatures. Two decisive factors were shown to effect the temperature-dependence. The first was EG between the excited triplet state and the emitting level of terbium(III) ion. The second was the EB accompanying the FET and BET. These EB are directly related to the re-orientation energy originated from the difference between the starting structures of the complexes and the final ones in the energy-transfer processes. When this difference is small, EB is also small. So, the temperature-dependence of the emission properties can be fully explained by EG. On the other hand, when this difference is large, the temperature-dependence of the emission is seriously affected by the competition between FET and BET. Then, an unusual behavior like a volcano-shaped temperature-dependence curve is observed. Quantum chemical calculations supported that the electron configurations of the ligands greatly change between the ground state and the excited triplet state especially in the case of hfa, which has electron-withdrawing $-CF_3$ groups. In this work, we showed a new strategy for the design of the terbium(III) complexes with desired emission properties.

This work was supported by a Grant-in-Aid for Scientific Research (No. 17750014) and a Grant-in-Aid for Scientific Research on Priority Areas (417) (No. 17029038) from MEXT of the Japanese government. One of the authors (S. Katagiri) expresses his special thanks for the center of excellence (21COE) program "Creation of Integrated EcoChemistry" of Osaka University.

References

1 G. A. Hebbink, L. Grave, L. A. Woldering, D. N. Reinhoudt, F. C. J. M. Van Veggel, *J. Phys. Chem. A* **2003**, *107*, 2483.

2 S. I. Klink, L. Grave, D. N. Reinhoudt, F. C. J. M. van Veggel, M. H. V. Werts, F. A. J. Geurts, J. W. Hofstraat, *J. Phys. Chem. A* **2000**, *104*, 5457.

3 S. I. Klink, G. A. Hebbink, L. Grave, F. C. J. M. van Veggel, D. N. Reinhoudt, L. H. Slooff, A. Polman, J. W. Hofstraat, *J. Appl. Phys.* **1999**, *86*, 1181.

4 S. I. Klink, G. A. Hebbink, L. Grave, P. G. B. O. Alink, F. C. J. M. van Veggel, M. H. V. Werts, *J. Phys. Chem. A* **2002**, *106*, 3681.

5 L. Ying, A. Yu, X. Zhao, Q. Li, D. Zhou, C. Huang, S. Umetani, M. Matasai, *J. Phys. Chem.* **1996**, *100*, 18387.

6 B. Yan, H. Zhang, S. Wang, J. Ni, *J. Photochem. Photobiol., A* **1998**, *116*, 209.

7 Y. Hasegawa, M. Yamamuro, Y. Wada, N. Kanehisa, Y. Kai, S. Yanagida, *J. Phys. Chem. A* **2003**, *107*, 1697.

8 Y. Wada, M. Sato, Y. Tsukahara, *Angew. Chem., Int. Ed.* **2006**, *45*, 1925.

9 K. Nakamura, Y. Hasegawa, Y. Wada, S. Yanagida, *Chem. Phys. Lett.* **2004**, *398*, 500.

10 a) E. J. Schimitschek, E. G. K. Schwarz, *Nature* **1962**, *196*, 832. b) H. Samelson, A. Lempicki, C. Brecher, V. Brophy, *Appl. Phys. Lett.* **1964**, *5*, 173. c) T. Kobayashi, S. Nakatsuka, T. Iwafuji, K. Kuriki, N. Imai, T. Nakamoto, C. D. Claude, K. Sasaki, Y. Koike, Y. Okamoto, *Appl. Phys. Lett.* **1997**, *71*, 2421. d) K. Kuriki, Y. Koike, Y. Okamoto, *Chem. Rev.* **2002**, *102*, 2347.

11 a) S. Shindo, *Low-Speed Wind Tunnel Testing Technique*, ed. by CORONA PUBLISHING CO., LTD., Tokyo Japan, **1992**, Chap. 1. b) Proceedings of MOSAIC International Workshop, Tokyo, Japan, **2003**, November 4–9. c) K. Mitsuo, K. Asai, A. Takahashi, H. Mizushima, *Meas. Sci. Technol.* **2006**, *17*, 1282. d) K. Mitsuo, K. Asai, M. Hayasaka, M. Kameda, *J. Visualization* **2003**, *6*, 321.

12 J. N. Demas, B. A. DeGraff, *J. Macromol. Sci., Chem.* **1988**, *A25*, 1189.

13 A. P. Zipp, L. Sacksteder, J. Streich, A. Cook, J. N. Demas, B. A. DeGraff, *Inorg. Chem.* **1993**, *32*, 5629.

14 R. V. Slone, J. T. Hupp, C. L. Stern, T. E. Albrecht-Schmitt, *Inorg. Chem.* **1996**, *35*, 4096.

15 K. Maruszewski, D. Andrzejewski, W. Strek, *J. Lumin.* **1997**, *72–74*, 226.

16 B. F. Carroll, J. P. Hubner, K. S. Schanze, J. M. Bedlek-Anslow, *J. Visualization* **2001**, *4*, 121.

17 G. Khalil, M. Gouterman, S. Ching, C. Costin, L. Coyle, S. Gouin, E. Green, M. Sadilek, R. Wan, J. Yearyean, B. Zelelow, *J. Porphyrins Phthalocyanines* **2002**, *6*, 135.

18 a) T. Gunnlaugsson, J. P. Leonard, K. Sénéchal, A. J. Harte, *J. Am. Chem. Soc.* **2003**, *125*, 12062. b) J. B. Beck, S. J. Rowan, *J. Am. Chem. Soc.* **2003**, *125*, 13922. c) R. K. Mahajan, I. Kaur, R. Kaur, S. Uchida, A. Onimaru, S. Shinoda, H. Tsukube, *Chem. Commun.* **2003**, 2238. d) S. Petoud, S. M. Cohen, J.-C. G. Bünzli, K. N. Raymond, *J. Am. Chem. Soc.* **2003**, *125*, 13324. e) P. B. Glover, P. R. Ashton, L. J. Childs, A. Rodger, M. Kercher, R. M. Williams, L. De Cola, Z. Pikramenou, *J. Am. Chem. Soc.* **2003**, *125*, 9918. f) T. Gunnlaugsson, J. P. Leonard, *Chem. Commun.* **2003**, 2424.

19 M. Mitsuishi, S. Kikuchi, T. Miyashita, Y. Amao, *J. Mater.*

Chem. **2003**, *13*, 2875.
20 G. E. Khalil, K. Lau, G. D. Phelan, B. Carlson, M. Gouterman, J. B. Callis, L. R. Dalton, *Rev. Sci. Instrum.* **2004**, *75*, 192.
21 S. Katagiri, Y. Hasegawa, Y. Wada, S. Yanagida, *Chem. Lett.* **2004**, *33*, 1438.
22 J. Yu, *J. Lumin.* **1998**, *78*, 265.
23 a) G. L. Closs, P. Piotrowiak, J. M. MacInnis, G. R. Fleming, *J. Am. Chem. Soc.* **1988**, *110*, 2652. b) G. L. Closs, M. D. Johnson, J. R. Miller, P. Piotrowiak, *J. Am. Chem. Soc.* **1989**, *111*, 3751.
24 D. L. Dexter, *J. Chem. Phys.* **1953**, *21*, 836.
25 S. Sato, M. Wada, *Bull. Chem. Soc. Jpn.* **1970**, *43*, 1955.
26 L. Liu, W. Li, Z. Hong, J. Peng, X. Liu, C. Liang, Z. Liu, J. Yu, D. Zhao, *Synth. Met.* **1997**, *91*, 267.
27 L. R. Melby, N. J. Rose, E. Abramson, J. C. Caris, *J. Am. Chem. Soc.* **1964**, *86*, 5117.
28 M. Latva, H. Takalo, V. M. Mukkala, C. Matachescu, J. C. Rodriguez-Ubis, J. Kankare, *J. Lumin.* **1997**, *75*, 149.
29 Y. Hasegawa, M. Iwamuro, K. Murakoshi, Y. Wada, R. Arakawa, T. Yamanaka, N. Nakashima, S. Yanagida, *Bull. Chem. Soc. Jpn.* **1998**, *71*, 2573.
30 Y. Hasegawa, T. Ohkubo, K. Sogabe, Y. Kawamura, Y. Wada, N. Nakashima, S. Yanagida, *Angew. Chem., Int. Ed.* **2000**, *39*, 357.
31 F. Gan, *Laser Materials*, World Scientific, Singapore, **1995**, p. 70.
32 F. Gutierrez, C. Tedeschi, L. Maron, J. P. Daudey, R. Poteau, J. Azema, P. Tisnes, C. Picard, *Dalton Trans.* **2004**, 1334.